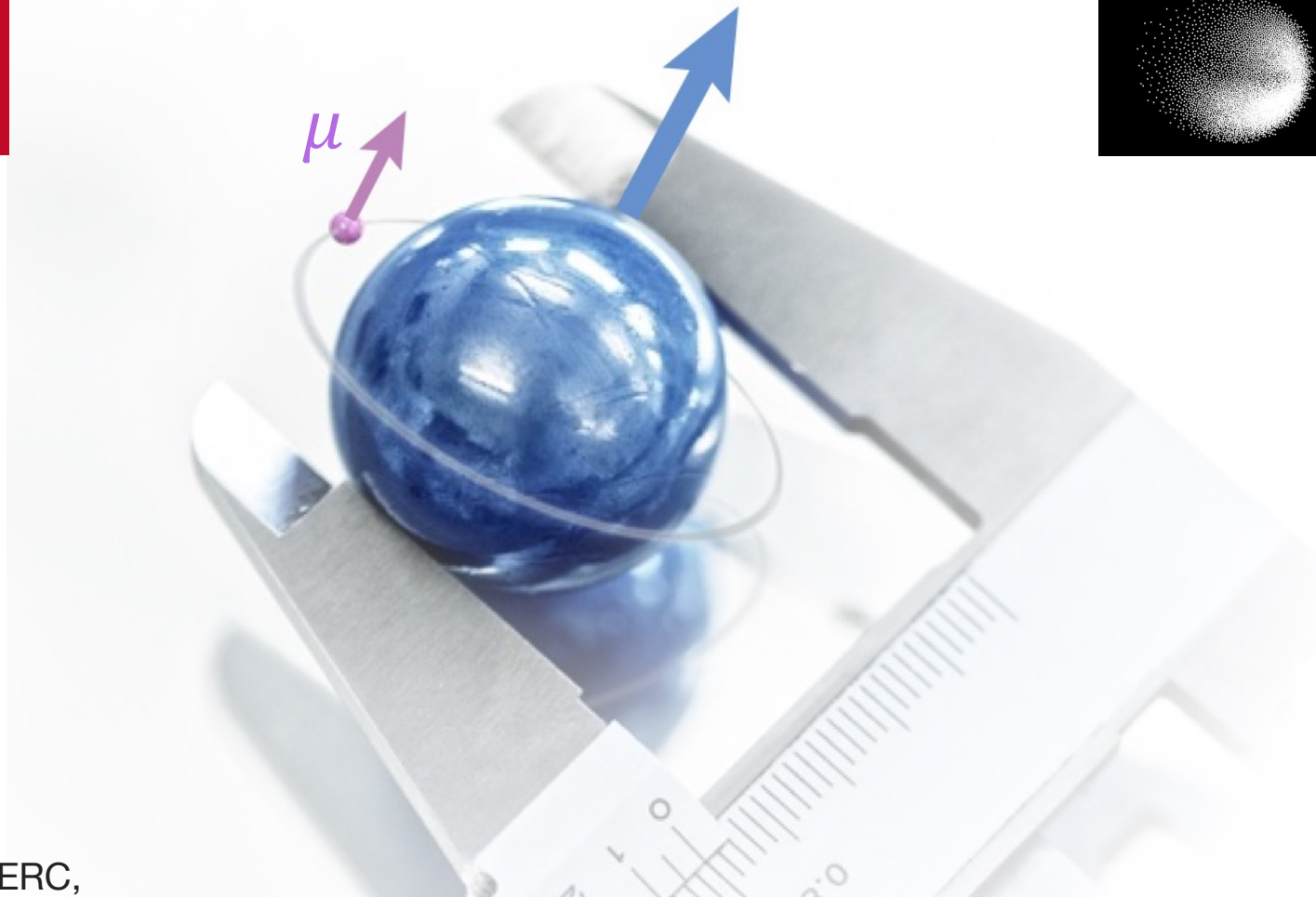
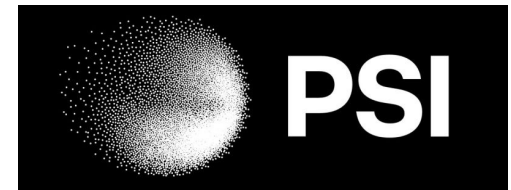


Hyperfine splitting in muonic hydrogen

AG Pohl

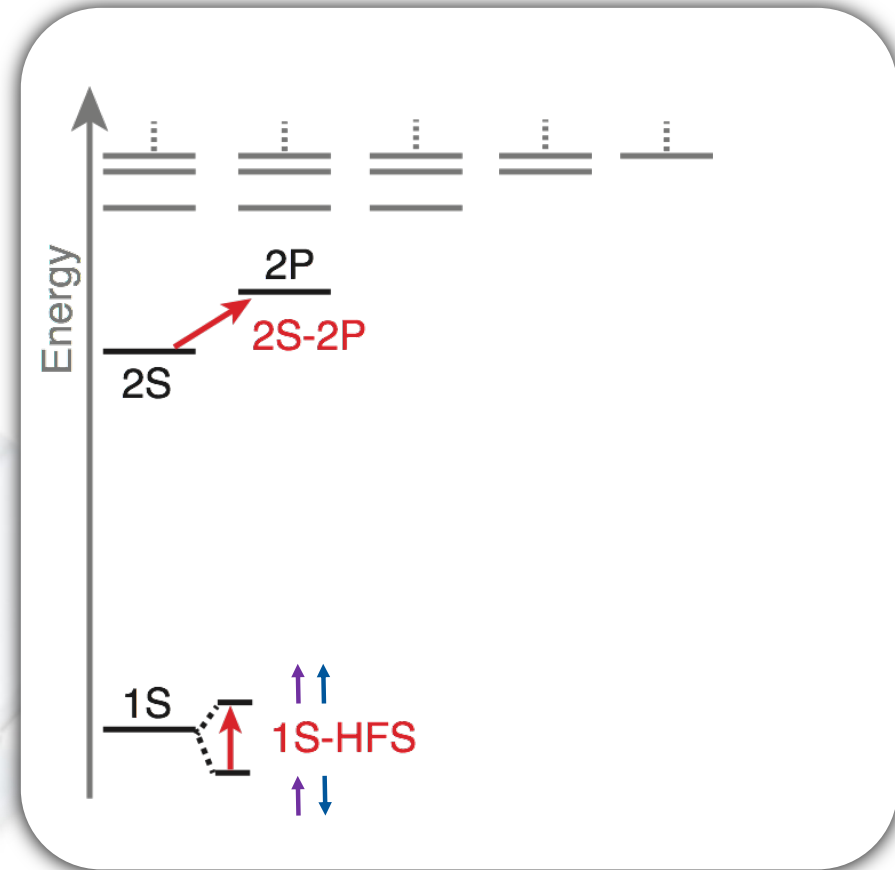
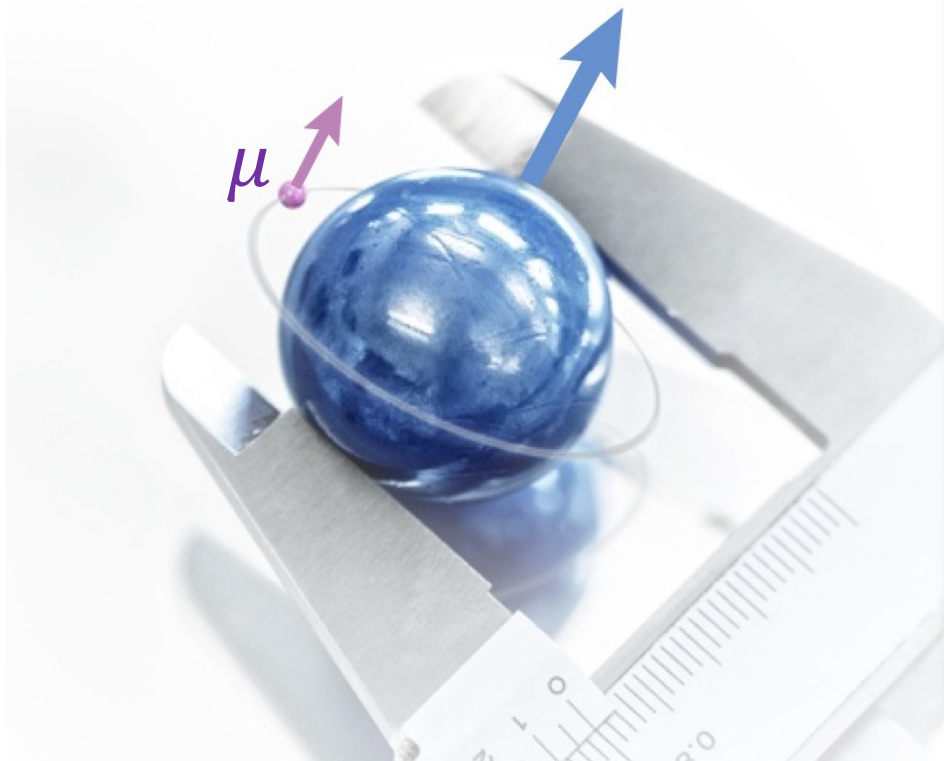


CREMA
collaboration



Supported by ERC,
SNF, DFG

Goal

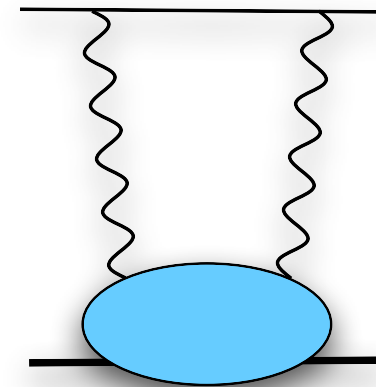
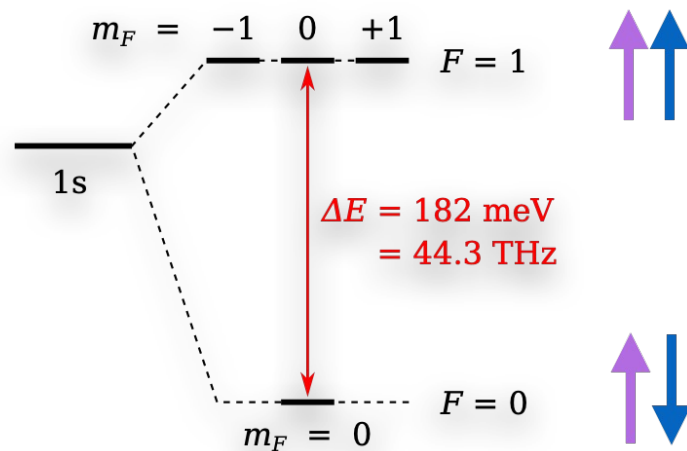


Measure the 1s-HFS in μp with a relative accuracy $\delta \approx 1 \times 10^{-6}$

1S hyperfine splitting in muonic hydrogen

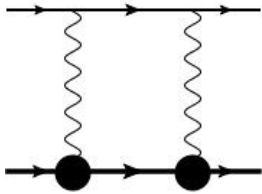
$$E_{1S\text{-HFS}}(\mu\text{H}) = \underbrace{[182.443]}_{E_F} + \underbrace{[1.350(7)]}_{\text{QED+weak}} + \underbrace{[0.004]}_{\text{hVP}} - \underbrace{1.30653(17) \left(\frac{r_{Zp}}{\text{fm}}\right) + E_F(1.01656(4)\Delta_{\text{recoil}} + 1.00402\Delta_{\text{pol}})}_{2\gamma \text{ incl. radiative corr.}} \text{meV}$$

Antognini, Hagelstein, Pascalutsa, Annual reviews 389, 418 (2022)

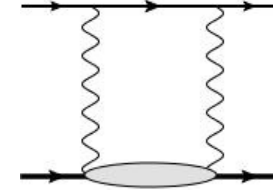


Extract the nuclear structure contribution with $\approx 1 \times 10^{-4}$ relative accuracy

Proton structure dependent contributions



$$E_{nS\text{-HFS}}^{(2\gamma)} = \frac{E_F}{n^3} (\Delta_Z + \Delta_{\text{recoil}} + \Delta_{\text{pol}}).$$



Zemach

$$\Delta_Z = -2Z\alpha m_r r_Z \quad r_Z = -\frac{4}{\pi} \int_0^\infty \frac{dQ}{Q^2} \left[\frac{G_E(Q^2)G_M(Q^2)}{1 + \kappa_N} - 1 \right].$$

$$\Delta_Z (\mu\text{H}) = -7403_{-16}^{+21} \text{ ppm}$$

Lin, Yong-Hui, Hammer, Meißner (2022)

Recoil

$$\Delta_{\text{recoil}} = \frac{Z\alpha}{\pi(1 + \kappa)} \int_0^\infty \frac{dQ}{Q} \left\{ \frac{8mM G_M(Q^2)}{v_l + v} \frac{G_M(Q^2)}{Q^2} \left(2F_1(Q^2) + \frac{F_1(Q^2) + 3F_2(Q^2)}{(v_l + 1)(v + 1)} \right) - \frac{8m_r G_M(Q^2)G_E(Q^2)}{Q} - \frac{m}{M} \frac{5 + 4v_l}{(1 + v_l)^2} F_2^2(Q^2) \right\}.$$

$$\Delta_{\text{recoil}} = 837.6_{-1.0}^{+2.8} \text{ ppm}$$

Antognini, Yong-Hui, Hammer, Meißner(2022)

Polarizability

$$\Delta_{\text{pol}} = \Delta_1 + \Delta_2 \equiv \frac{Z\alpha m}{2\pi(1 + \kappa_N)M} [\delta_1 + \delta_2],$$

$$\delta_1 = 18 \int_0^\infty \frac{dQ}{Q} \kappa_0(Q^2) I_1^{(\text{pol})}(Q^2) + 16M^4 \int_0^\infty \frac{dQ}{Q^3} \int_0^{x_0} dx \kappa_1(x, Q^2) g_1(x, Q^2),$$

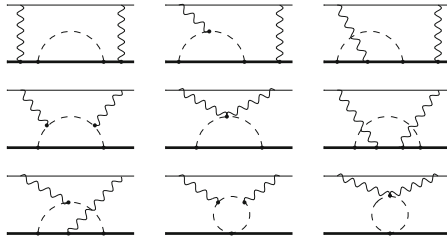
$$\delta_2 = 96M^2 \int_0^\infty \frac{dQ}{Q^3} \int_0^{x_0} dx \kappa_2(x, Q^2) g_2(x, Q^2),$$

$$\Delta_{\text{pol}} = 200.6(54) \text{ ppm}$$

Carlson et al. 2024

Proton polarizability

Chiral Perturbation theory



$$\Delta_{pol} = 38(62) \text{ ppm}$$

Hagelstein, Pascalutsa (2023)

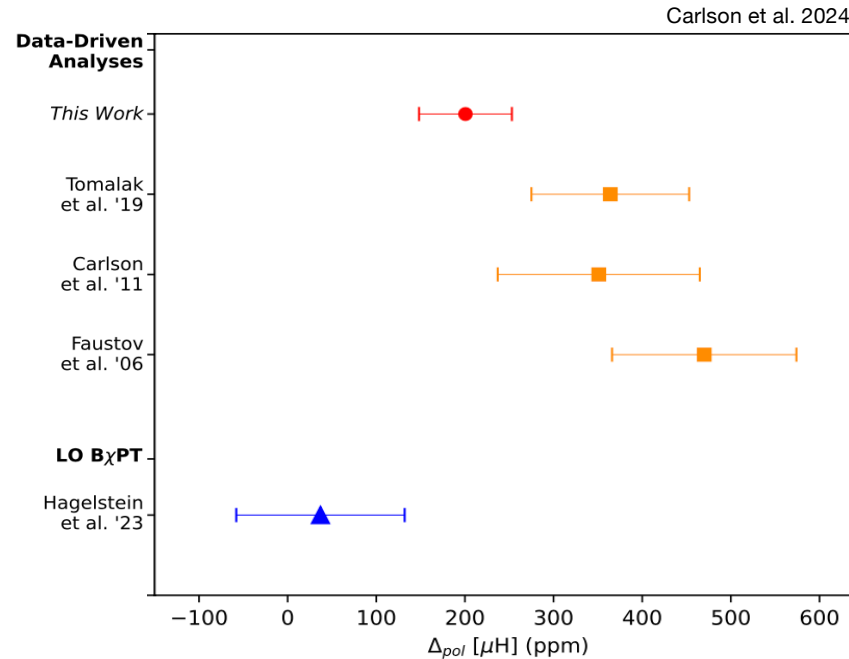
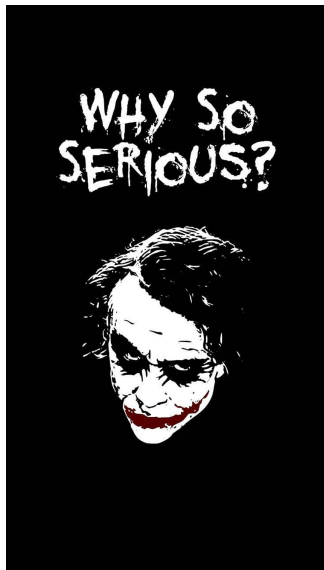
Dispersive analysis Data driven

Structure functions,
Form factors

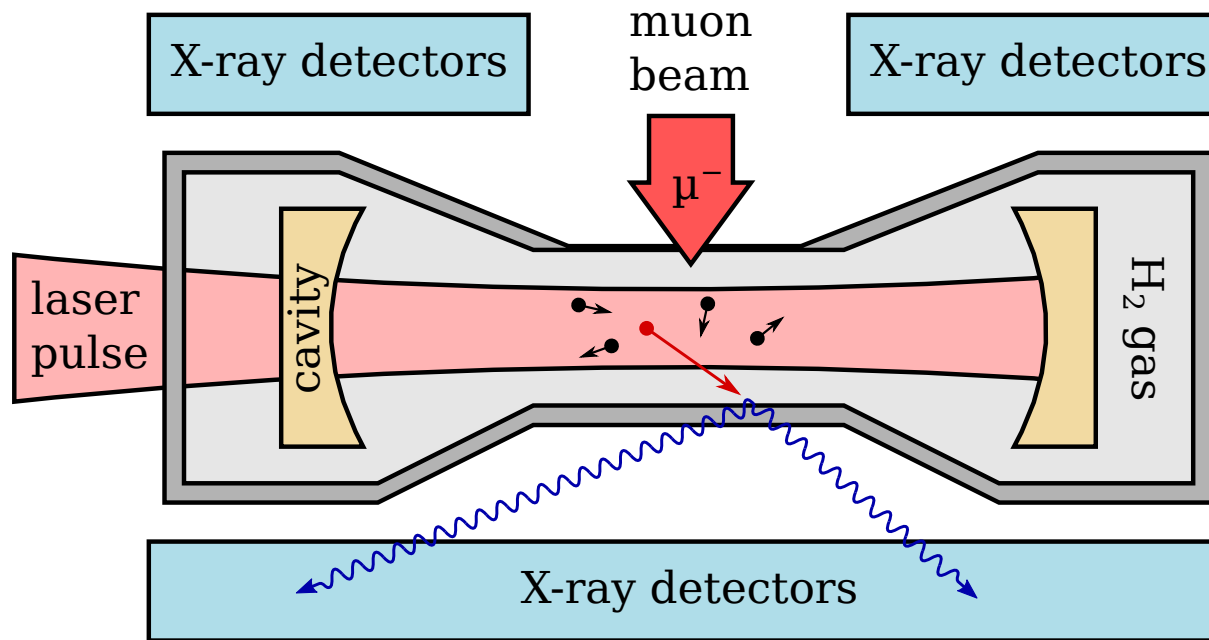
$$g_1(x, Q^2), g_2(x, Q^2), F_2 \dots$$

$$\Delta_{pol} = 200.6(54) \text{ ppm}$$

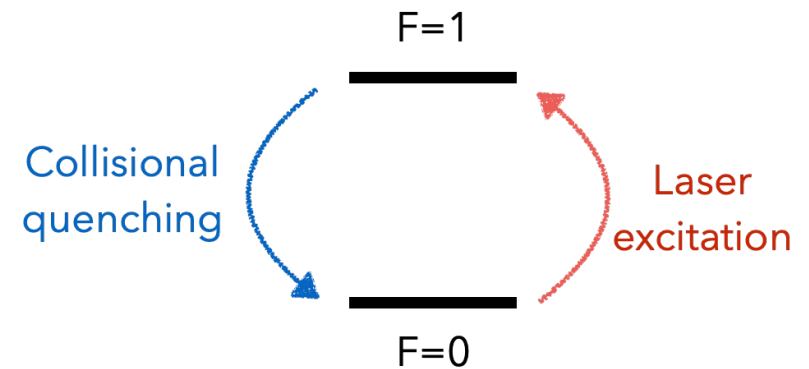
Carlson et al. 2024



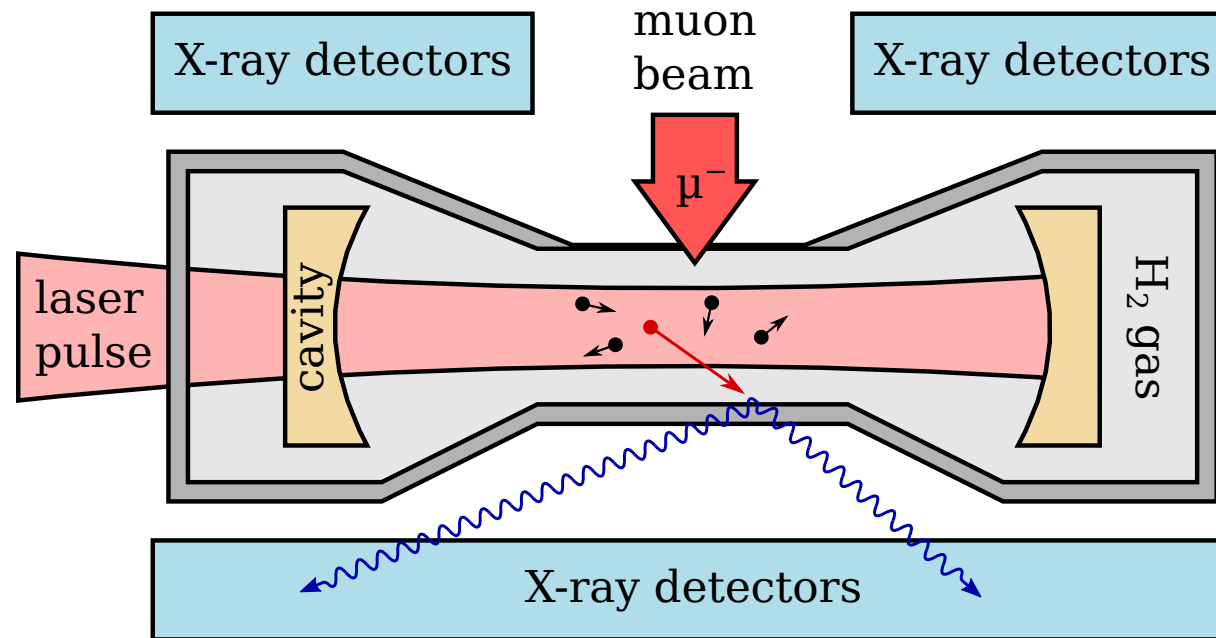
The principle of the experiment



- Stop muon beam in 1 mm H₂ gas target at 22 K, 0.5 bar
- Wait until μp atoms de-excite and thermalize
- Laser pulse: $\mu p(F=0) + \gamma \rightarrow \mu p(F=1)$
- De-excitation: $\mu p(F=1) + H_2 \rightarrow \mu p(F=0) + H_2 + E_{kin}$

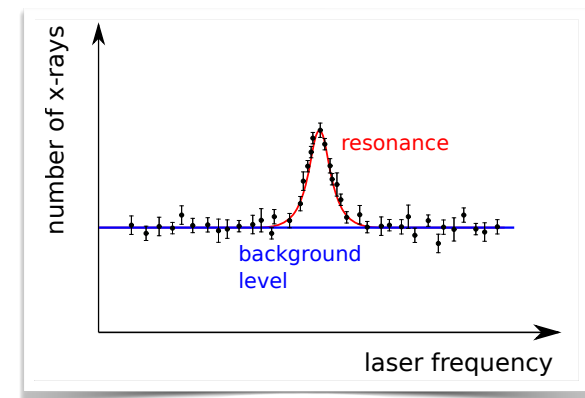


The principle of the experiment

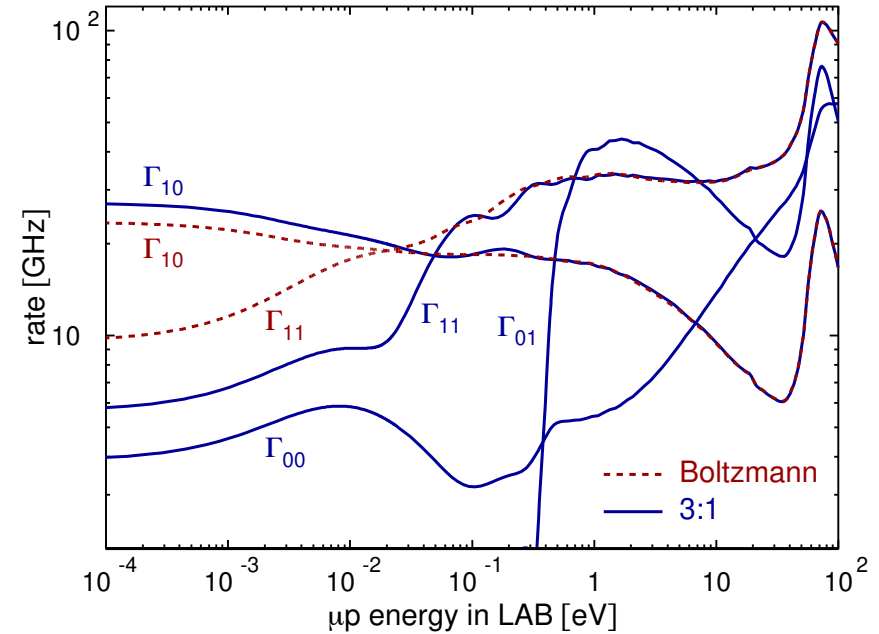
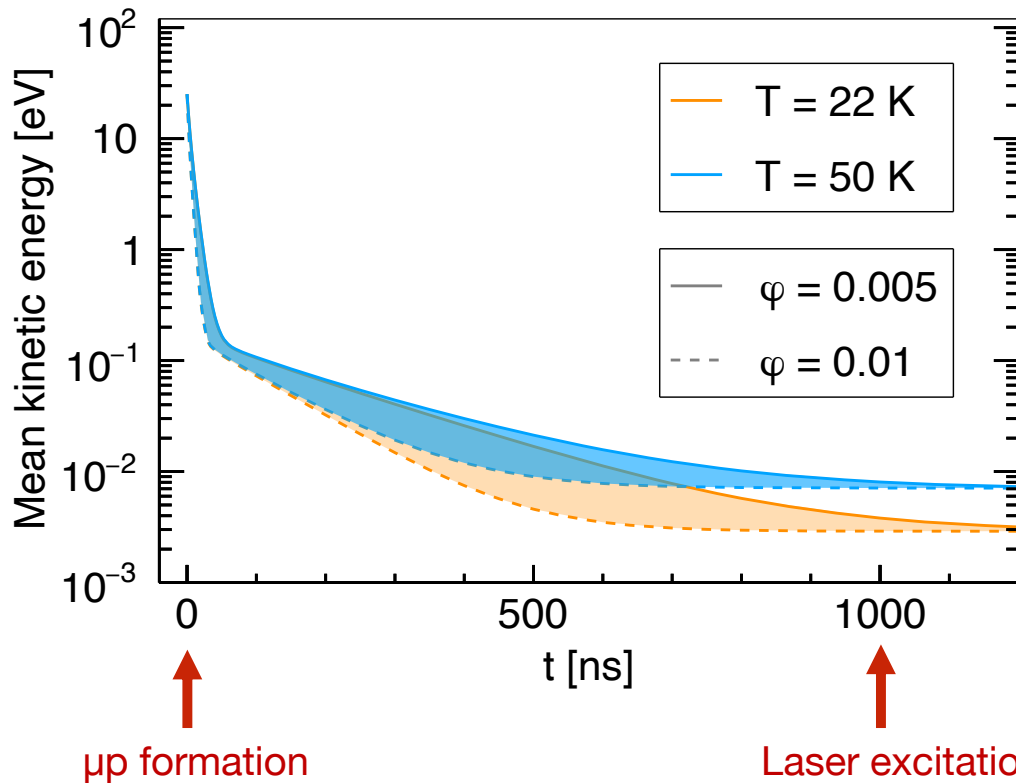
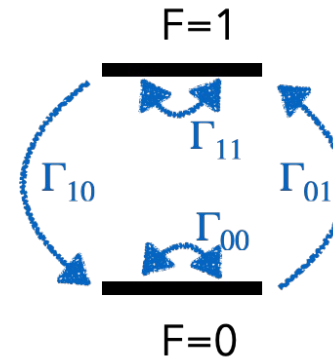
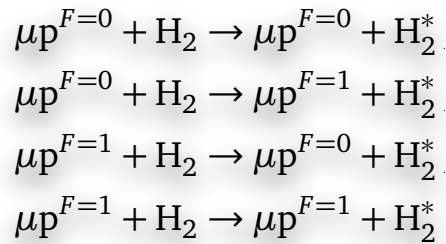


- Diffusion: μp diffuses to Au-coated target walls
- Detection: formed μAu^* de-excites producing X-rays
- Resonance: Plot number of X-ray events vs laser frequency

Related Proposals: FAMU at RIKEN/RAL, muonic H at J-PARC

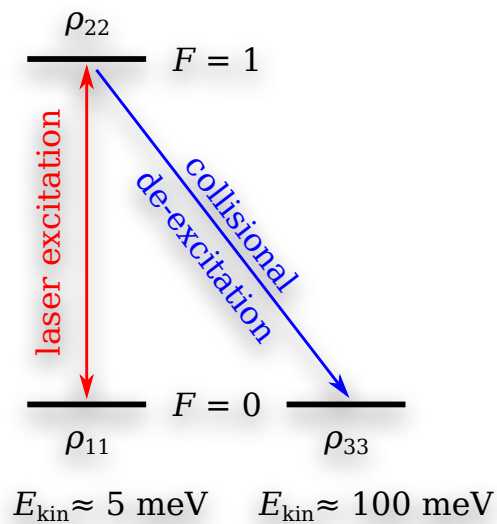


μp thermalization



J. Nuber, Scipost (August, 2023)

Laser excitation modeled including collision



$$\frac{d\rho_{11}}{dt}(t) = -\text{Im}(\Omega\rho_{12}e^{i\Delta t}) + \Gamma_{\text{sp}}\rho_{22},$$

$$\frac{d\rho_{22}}{dt}(t) = \text{Im}(\Omega\rho_{12}e^{i\Delta t}) - (\Gamma_i + \Gamma_{\text{sp}})\rho_{22},$$

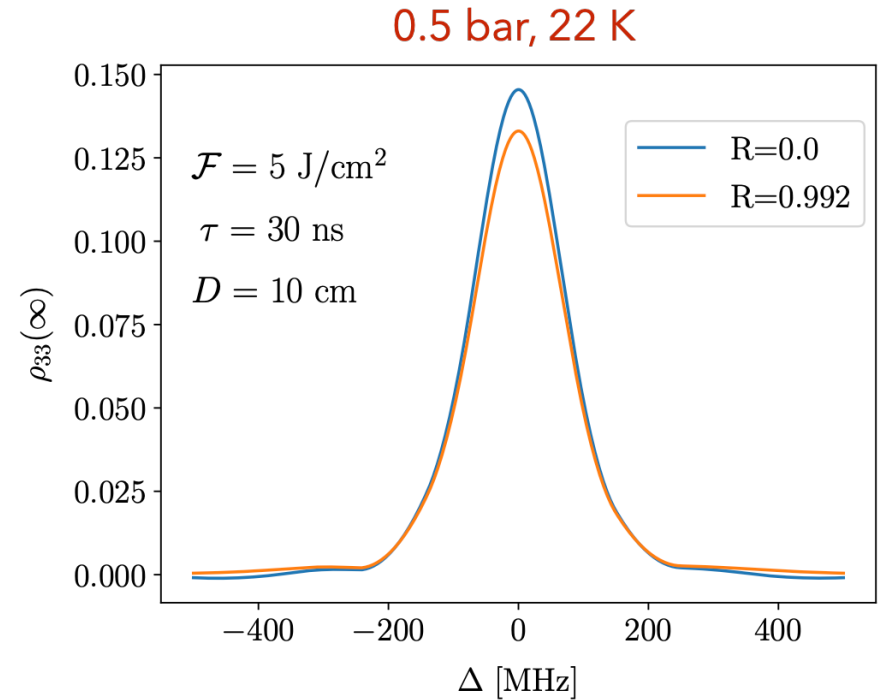
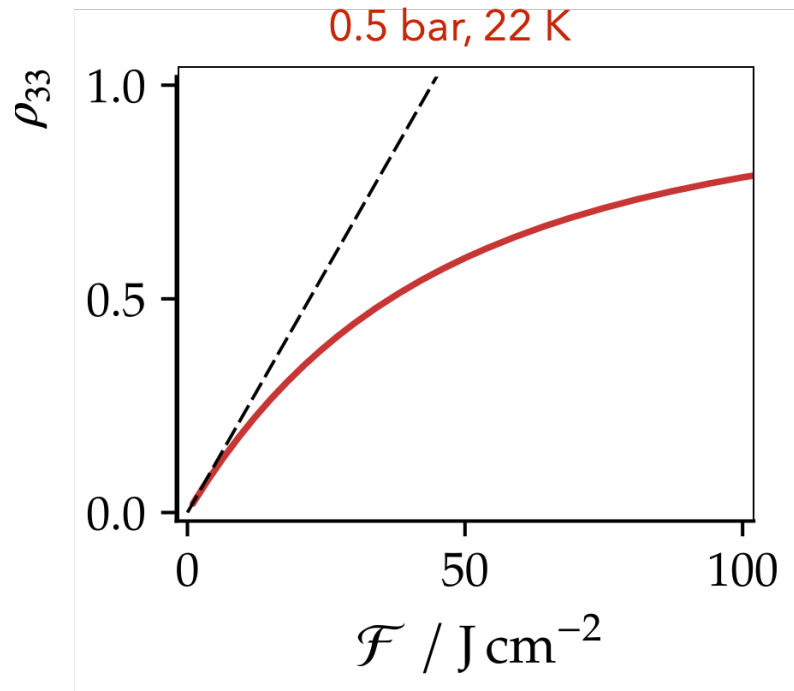
$$\frac{d\rho_{12}}{dt}(t) = \frac{i\Omega^*}{2}(\rho_{11} - \rho_{22})e^{-i\Delta t} - \frac{\Gamma_c}{2}\rho_{12},$$

$$\frac{d\rho_{33}}{dt}(t) = \Gamma_i\rho_{22},$$

- ✓ Inelastic collisions
- ✓ Elastic collisions
- ✓ Laser bandwidth
- ✓ Doppler broadening

P.Amaro et al. (scipost 2022)

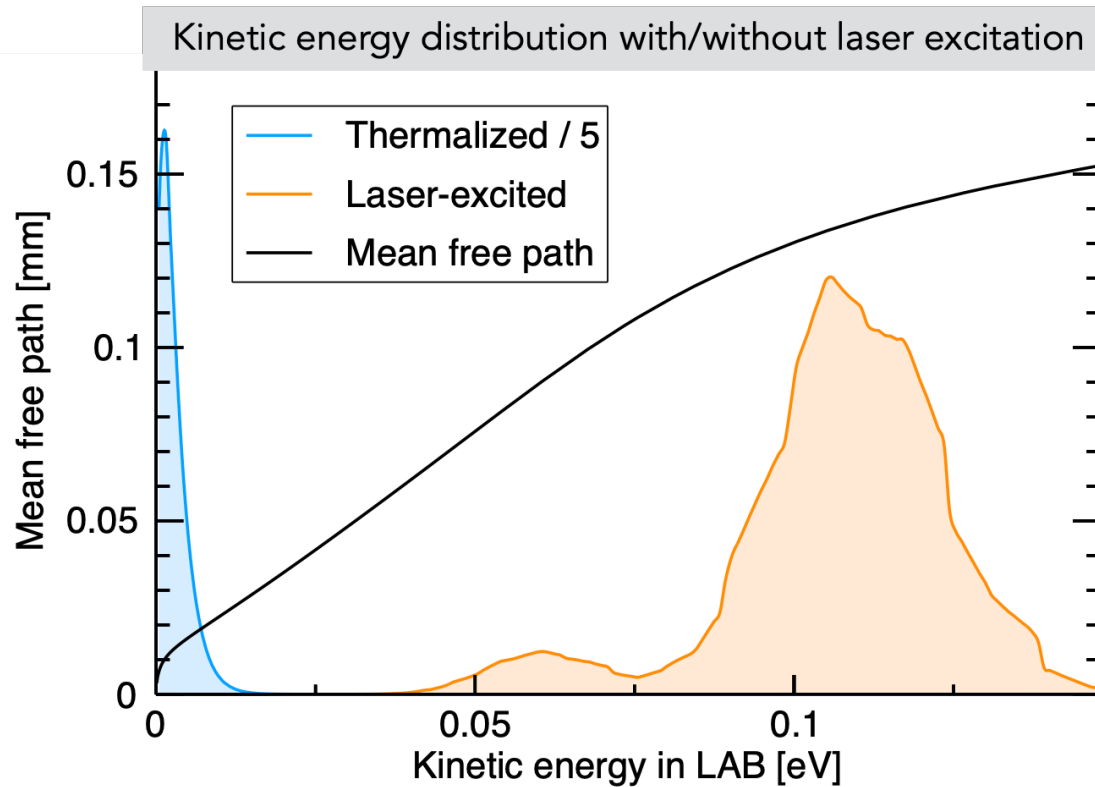
Saturation fluence and linewidth



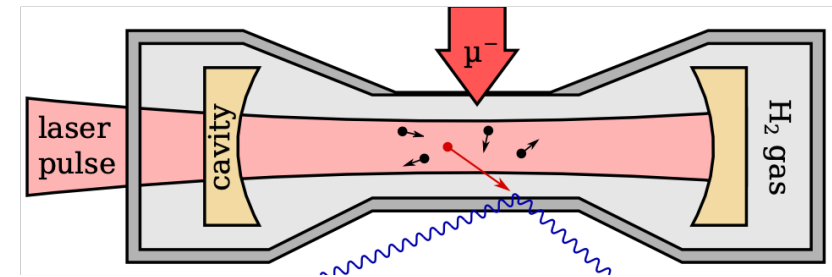
Transition	Linewidth	Saturation fluence
2S-2P	20 GHz	0.016 J/cm ²
HFS	200 MHz	44 J/cm ²

Thermalized vs laser excited atoms

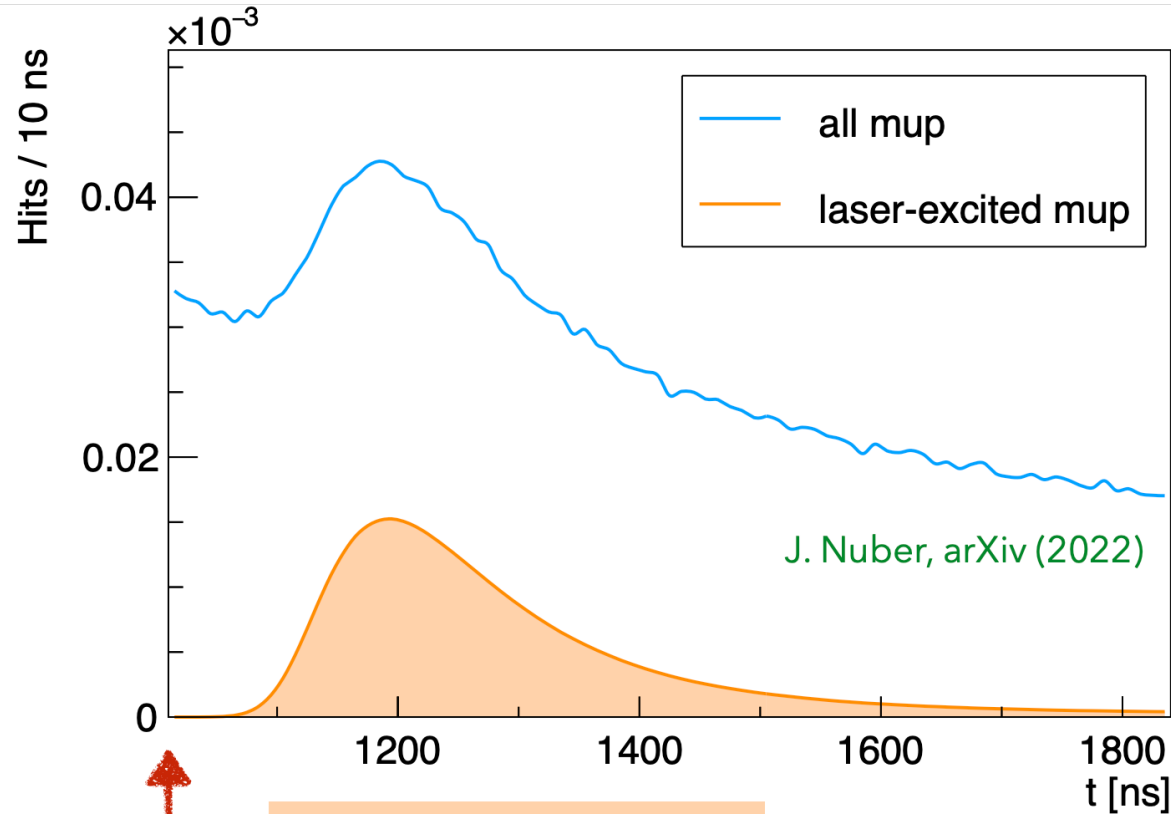
- ▶ De-excitation: $\mu\text{p}(F=1) + \text{H}_2 \rightarrow \mu\text{p}(F=0) + \text{H}_2 + E_{\text{kin}}$
- ▶ μp diffuses to Au-coated target walls



On average μp atoms wins 0.1 eV kinetic energy after a successful laser excitation



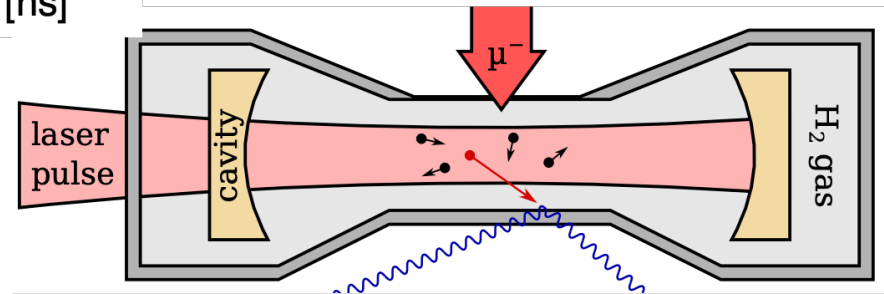
Diffusion to target walls



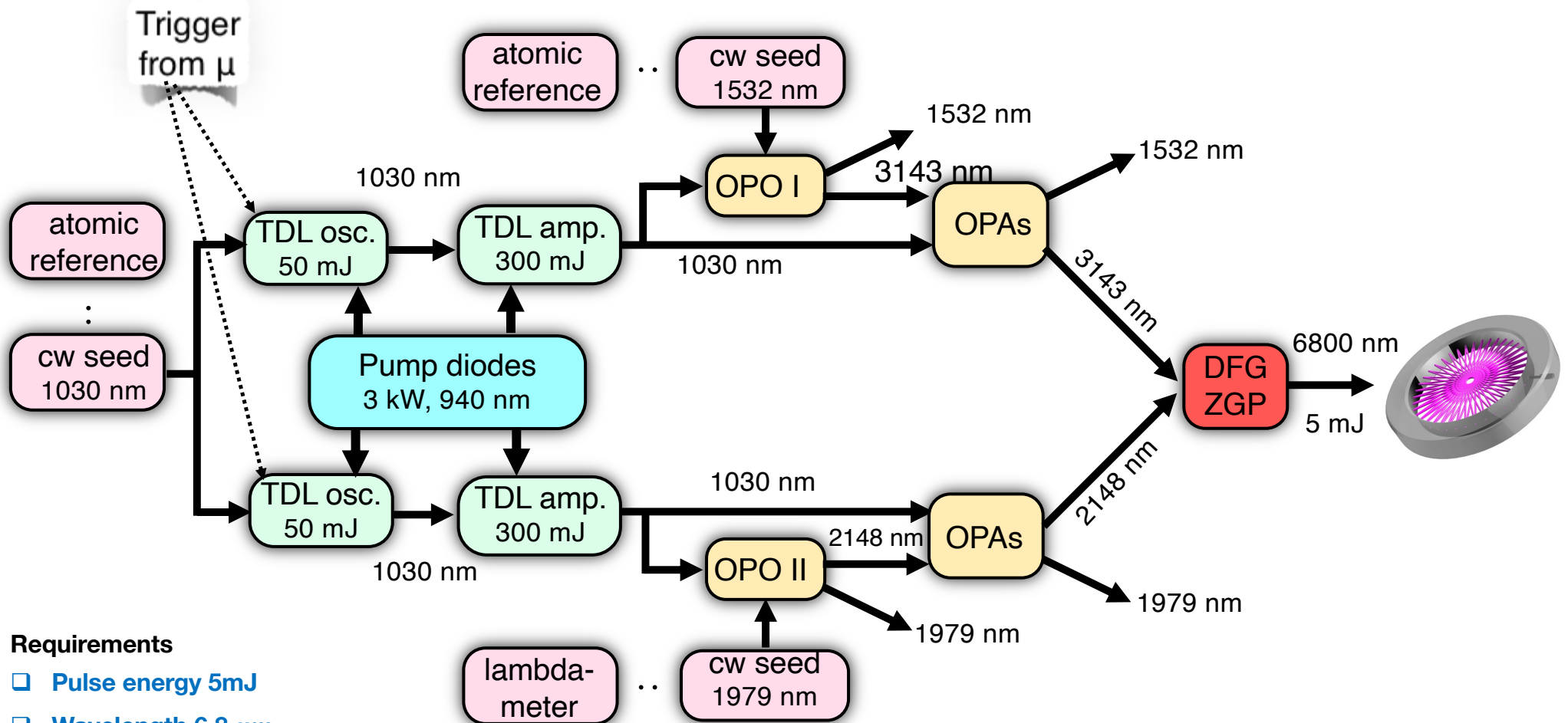
Event time window

Laser pulse

- ▶ 100 ns after laser excitation the first μp atoms reach the target walls
- ▶ Signal on top of a large background from μp atoms formed closed to the target walls



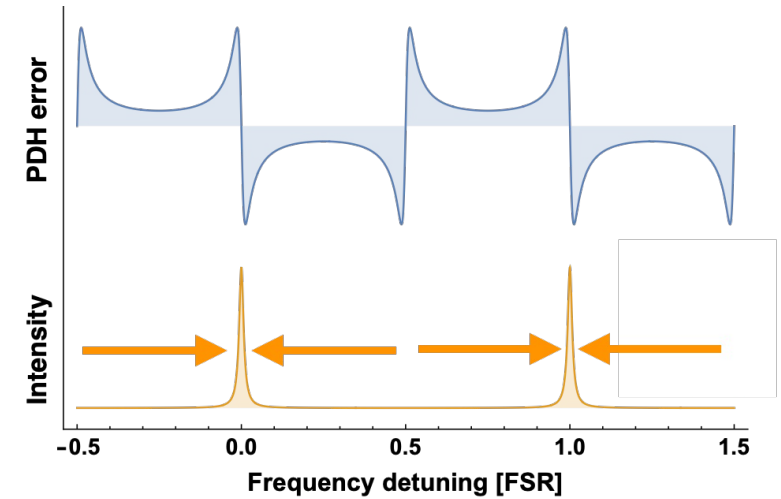
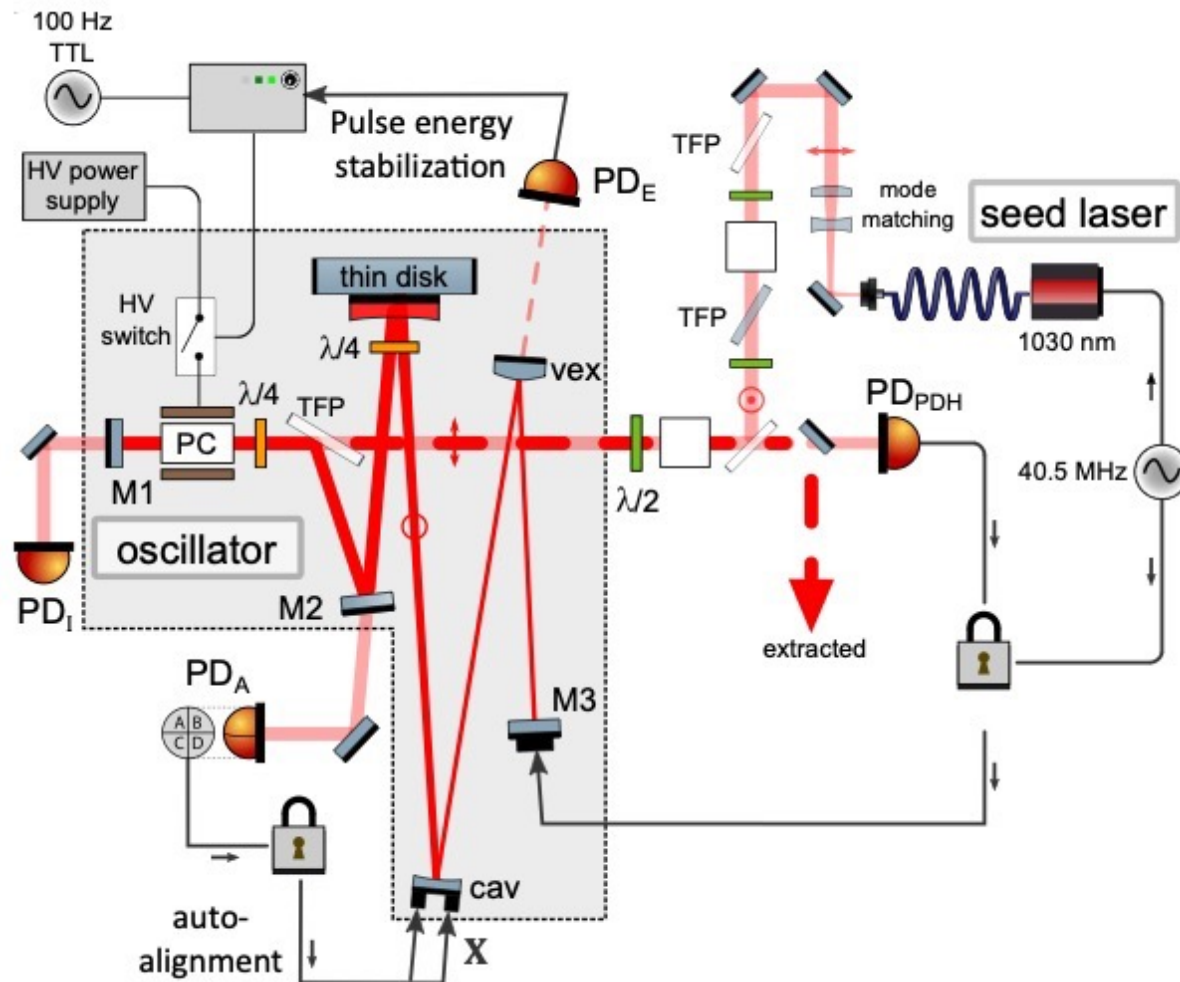
The laser system



Requirements

- Pulse energy 5mJ
- Wavelength 6.8 μm
- Linewidth < 100 MHz
- Stochastic trigger (detected muon)
- Response time 1 μs
- Tunability 40 GHz

Thin-disk oscillator



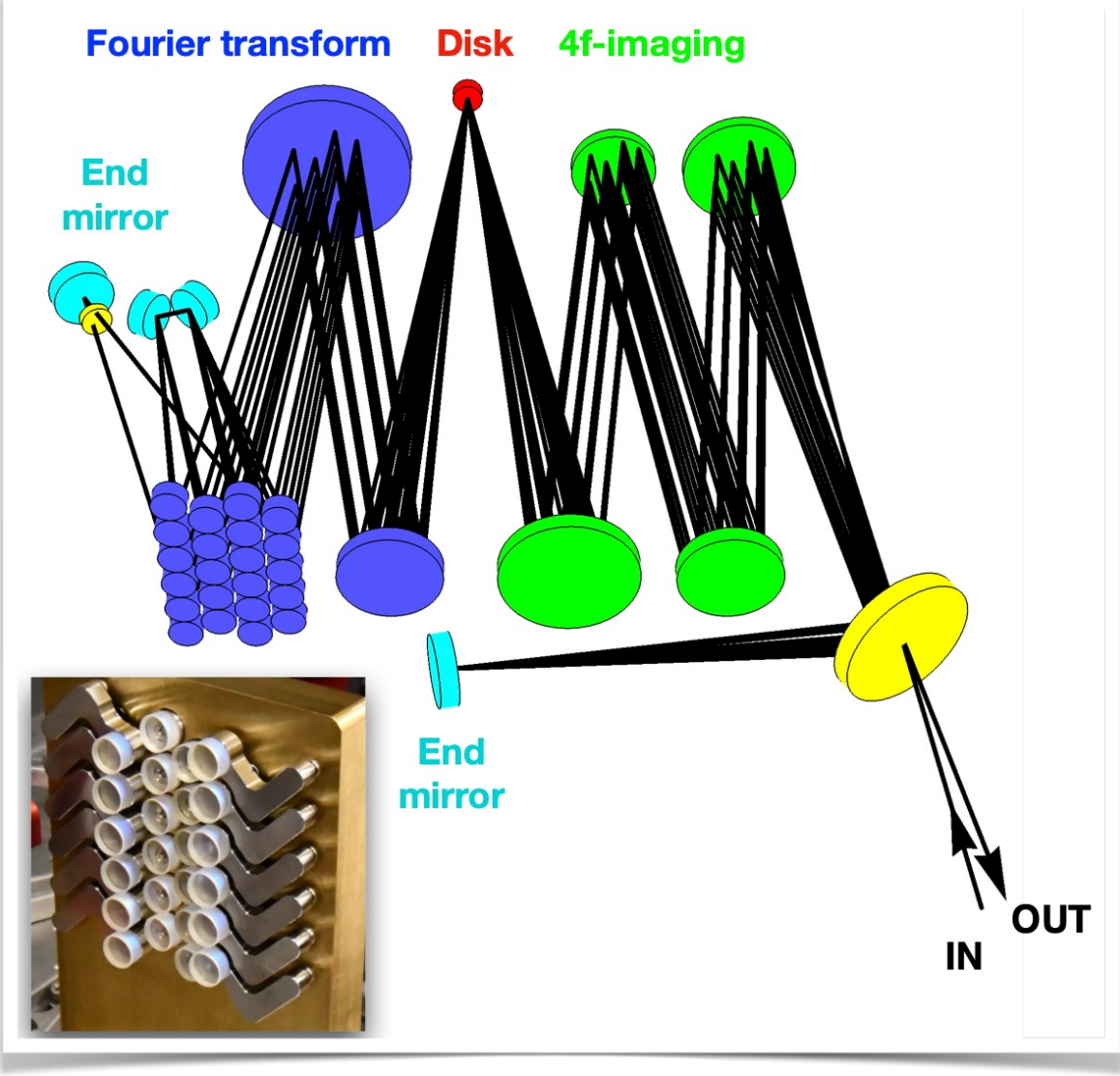
- ✓ Delay: 700 ns
- ✓ Energy: 50 mJ
- ✓ Pulse-to-pulse stability: <0.5% (rms)
- ✓ Single-frequency operation
- ✓ Laser chirp < 2 MHz
- ✓ PDH lock scheme with infinite dynamic range

Zeyen, Manuel, et al. review of scientific instruments 2023.

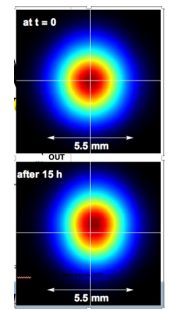
Zeyen, Manuel, et al. Optics express, 2023.

Multipass amplifier

Sequence
 4f
 amplification
 Fourier transform
 amplification
 4f
 4f
 amplification
 Fourier transform
 amplification
 4f
 4f
 amplification
 Fourier transform
 amplification
 4f
 4f
 .
 .
 .



- ✓ Insensitive to thermal lensing
- ✓ Energy: 330 mJ
- ✓ $M2 < 1.17$
- ✓ Pointing stability

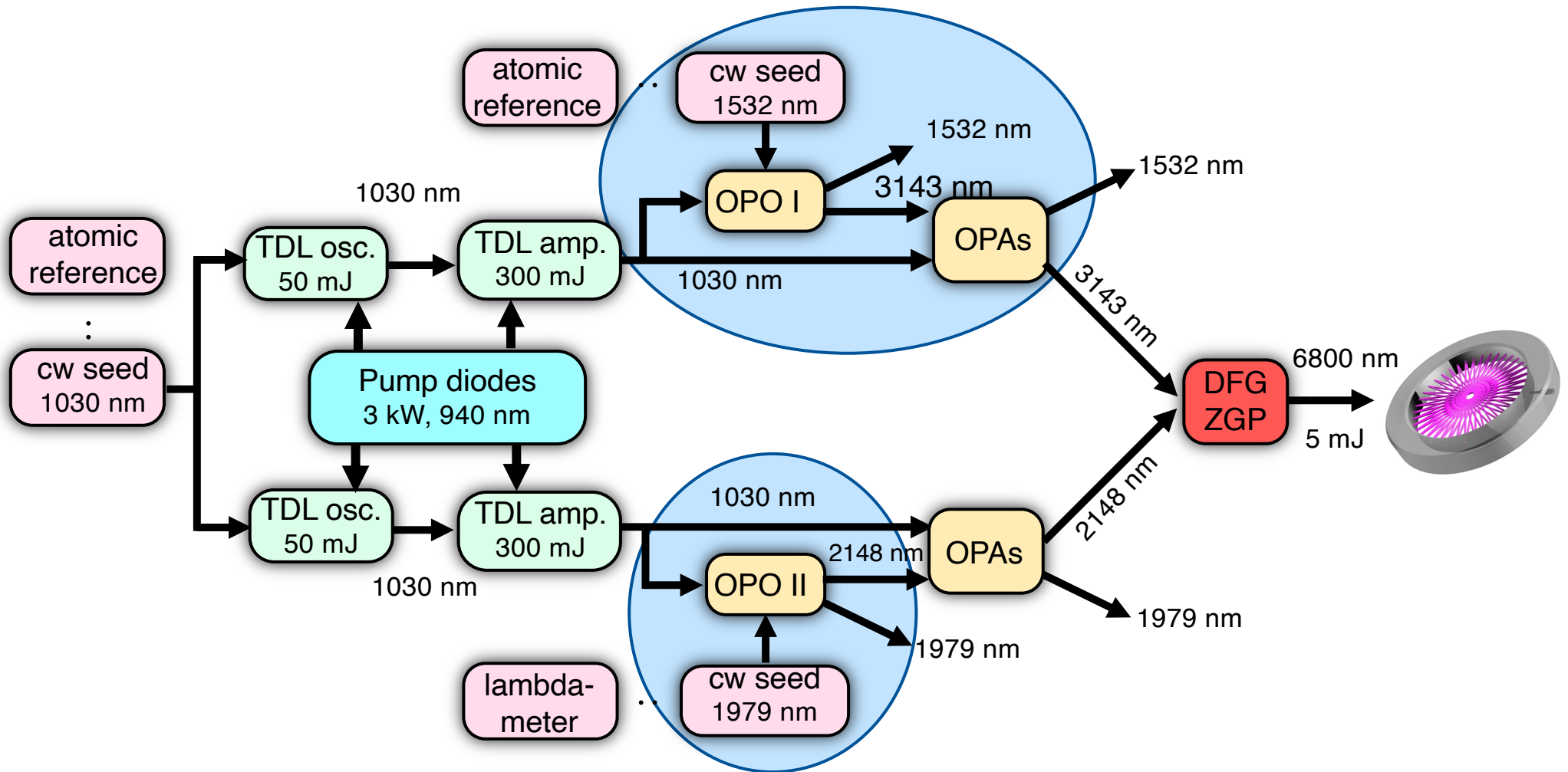


Zeyen, Manuel, et al. 2019

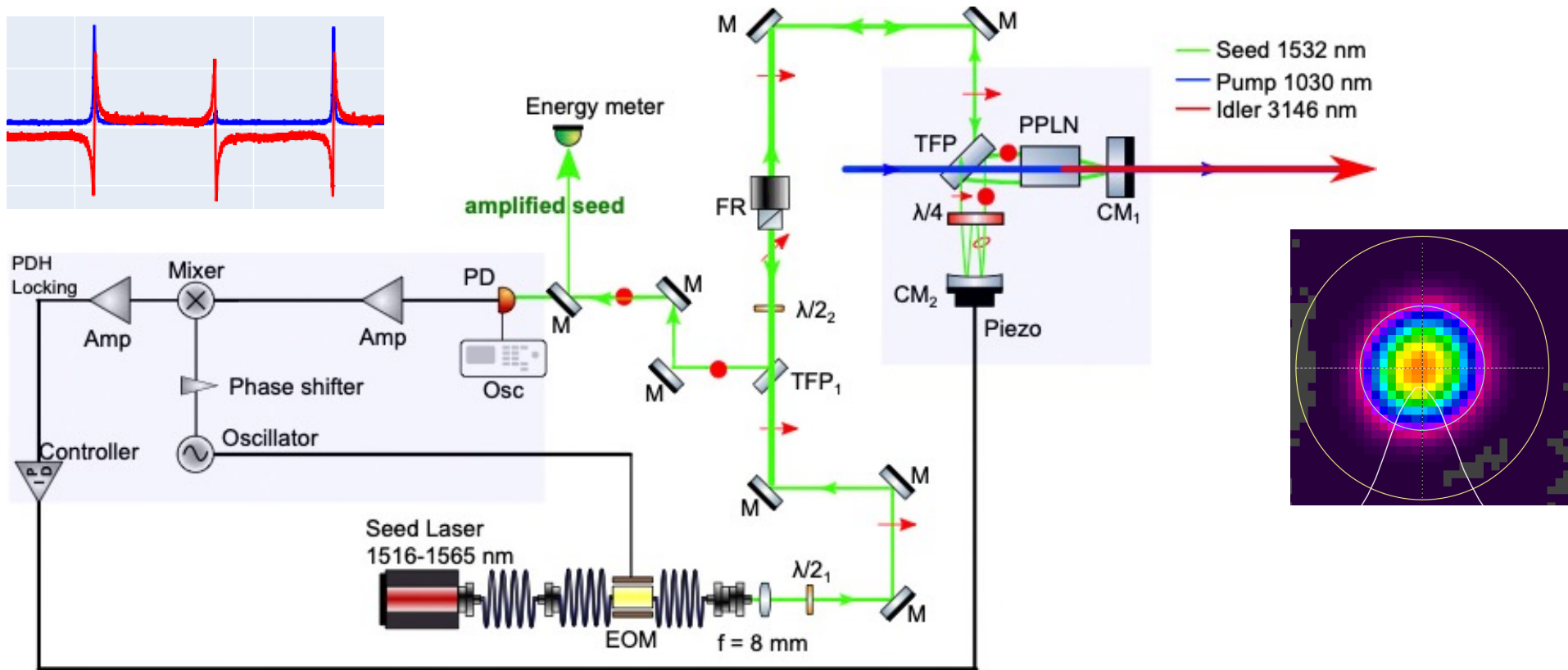
K. Schuhmann et al., Appl. Opt. 57, 10323-10333 (2018)

Zeyen, Manuel, et al. Optics express, 2024.

OPOs & OPAs

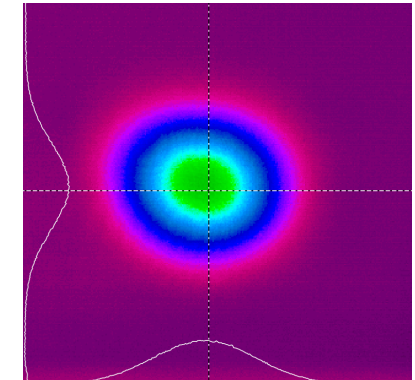
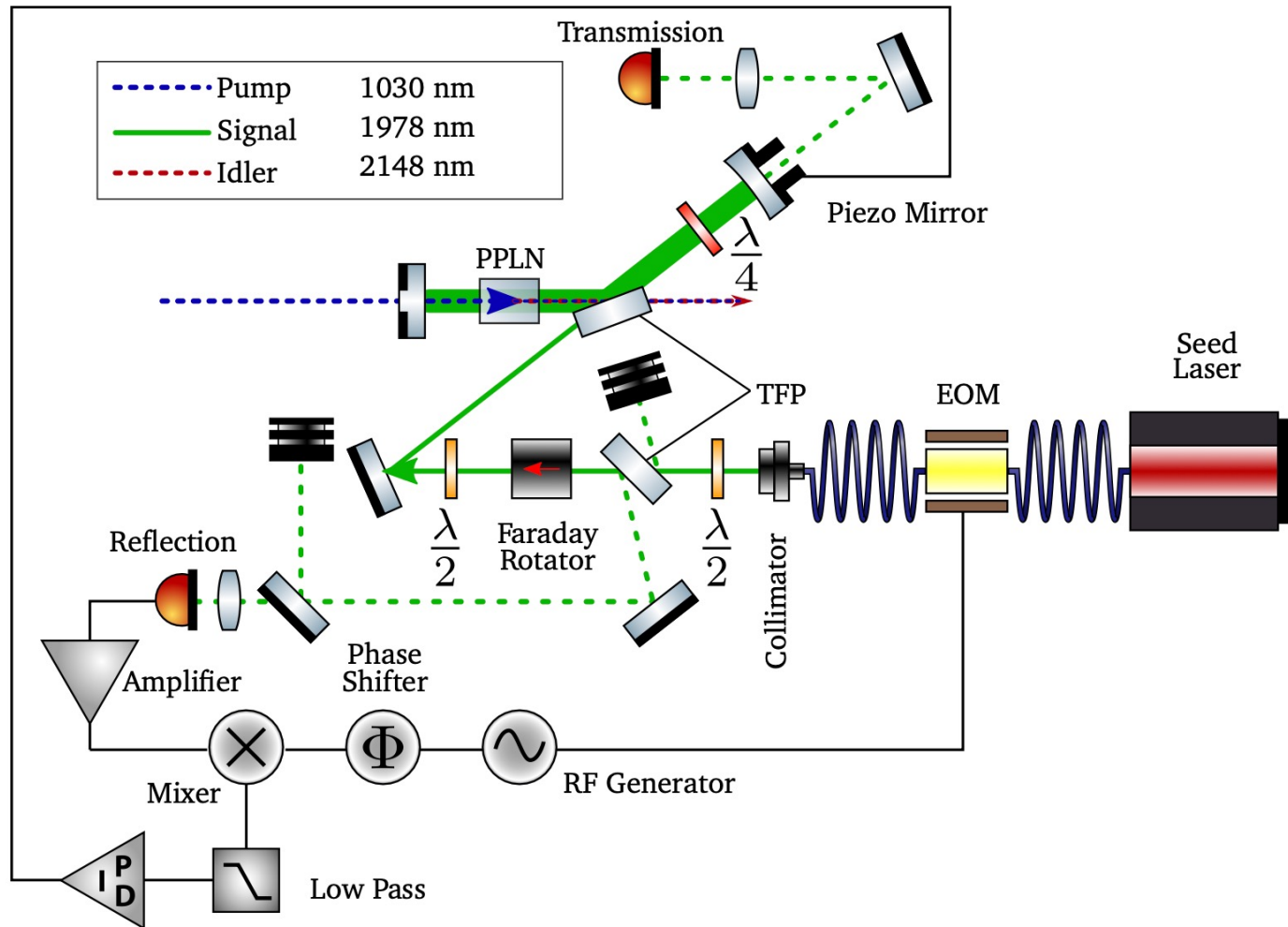


OPO & OPA @3146 nm



- ✓ Variable outcoupling cavity
- ✓ Infinite locking range (PDH locking)
- ✓ 3.3 mJ @ 3146 nm
- ✓ M2 = 1.01 (excellent beam quality)
- ✓ Pulse chirp < 2 MHz
- ✓ Rms energy stability < 2%
- ✓ Tunability of 2 nm

OPO & OPA @2148 nm

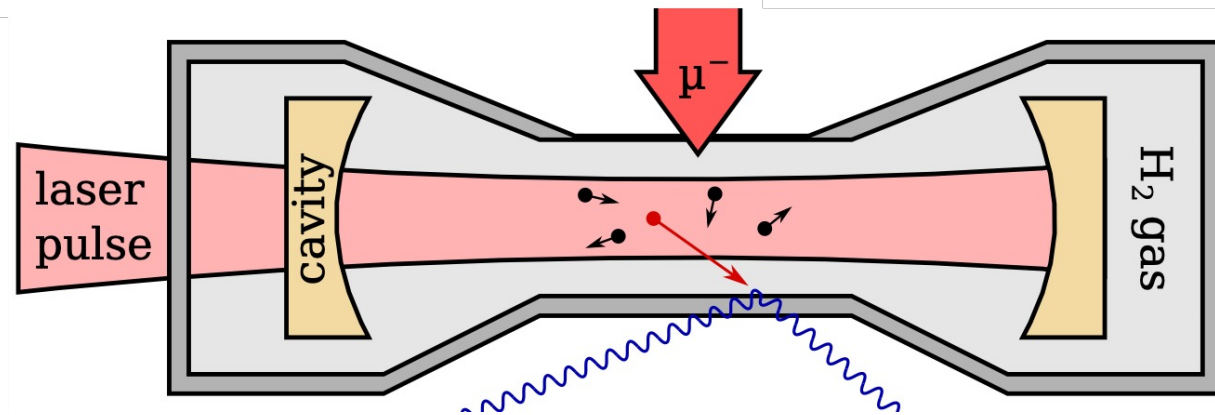
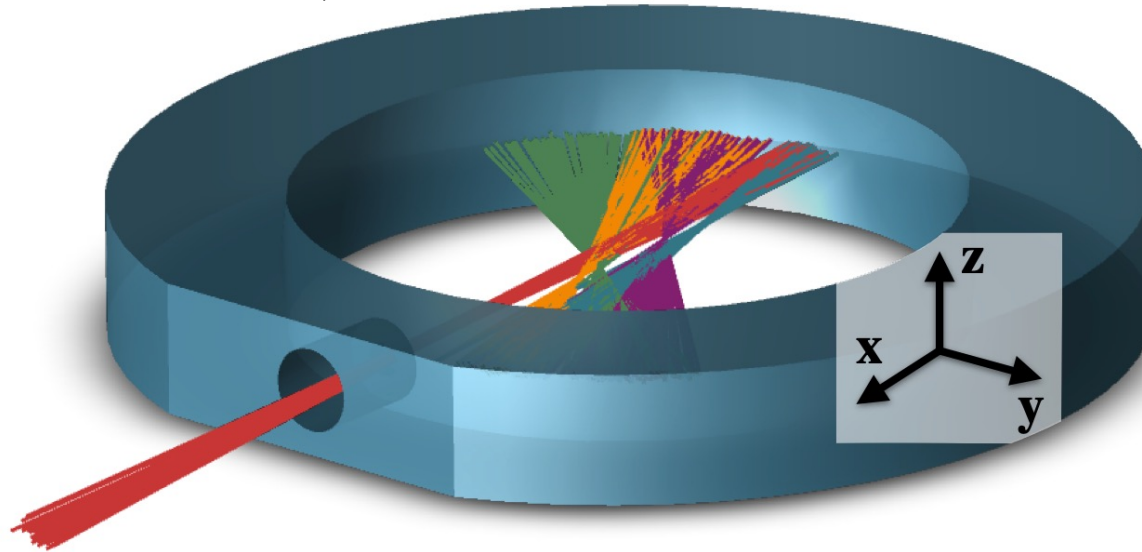


Preliminary

- ✓ 1.5 mJ @ 2148 nm
- ✓ Efficiency 40-50 %
- ✓ excellent beam quality
- ☐ OPA in preparation

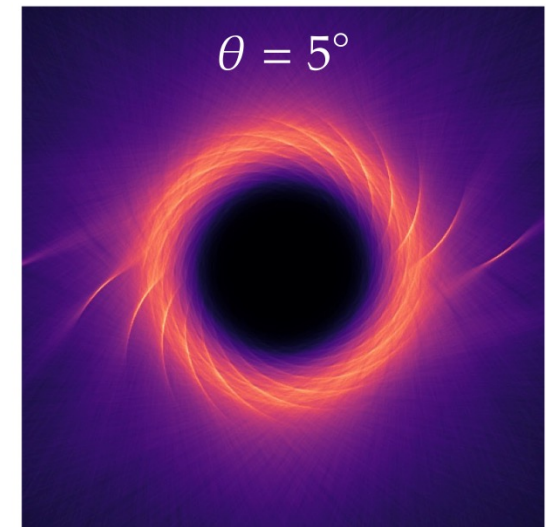
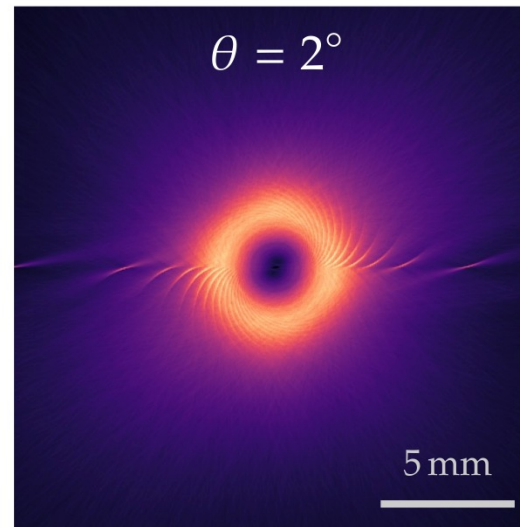
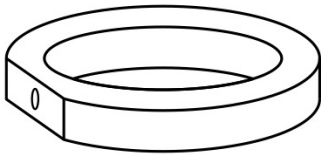
Enhancement cavity

— M. Marszalek, PhD Thesis, ETH 2022
M. Marszalek et.al, arXiv:2402.07223

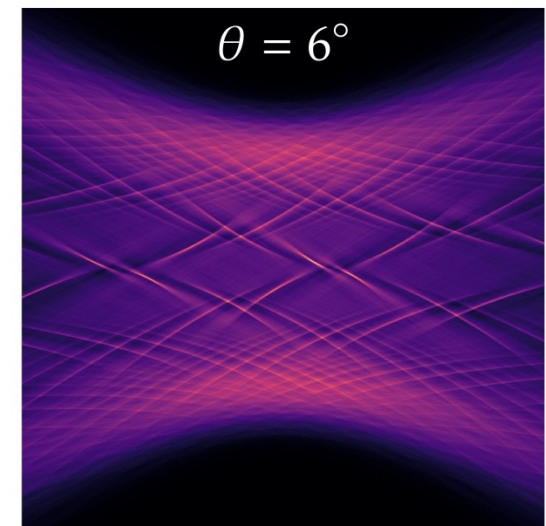
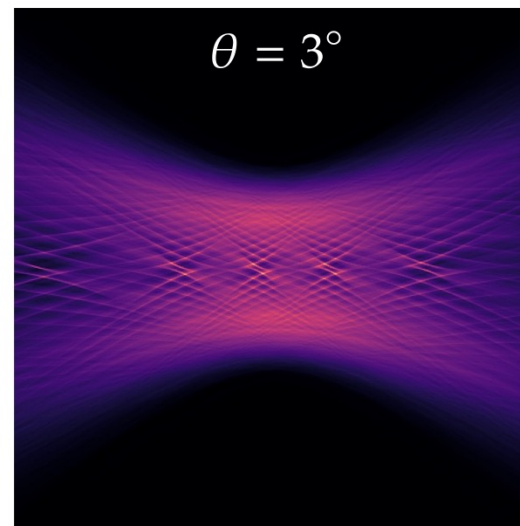
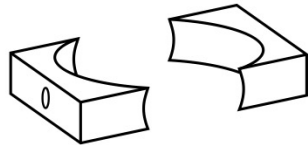


Two different configurations

- ▶ Resonant vertically
- ▶ Unstable horizontally

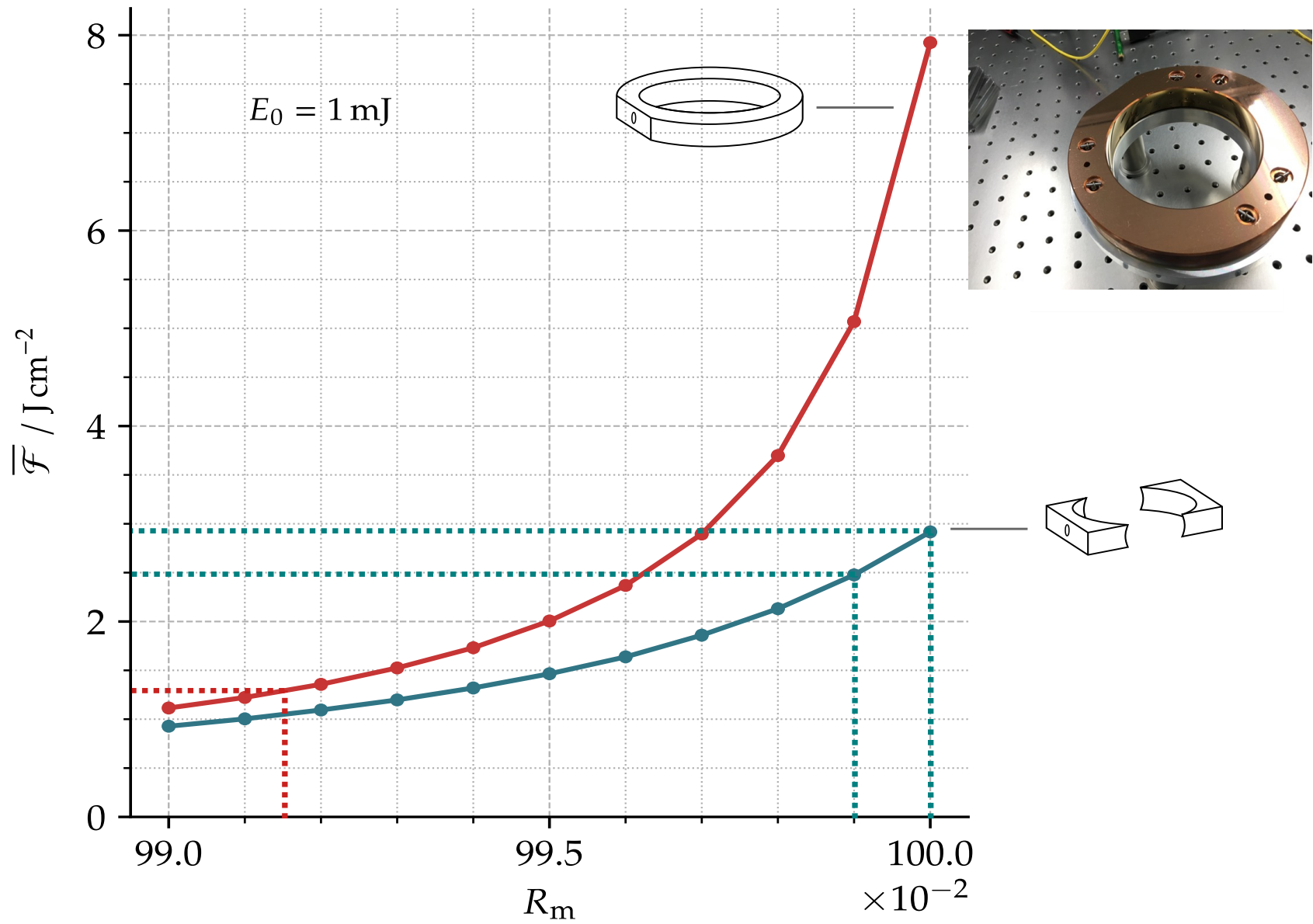


- ▶ Resonant vertically
- ▶ Stable horizontally

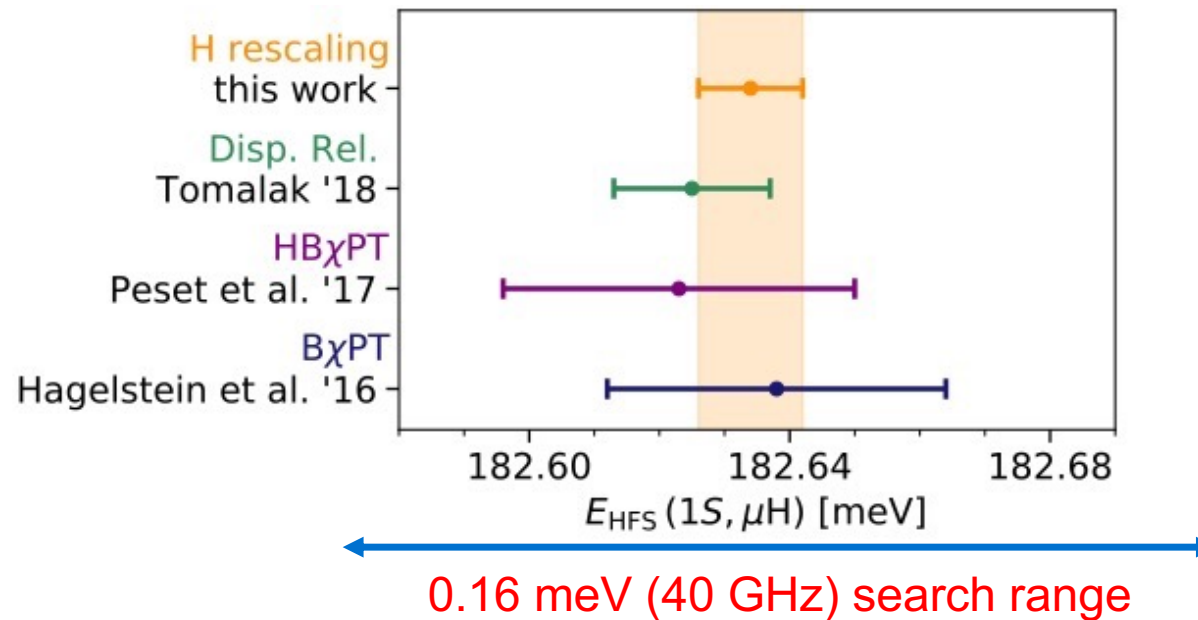


M. Marszalek , PhD Thesis, ETH 2022

Comparison

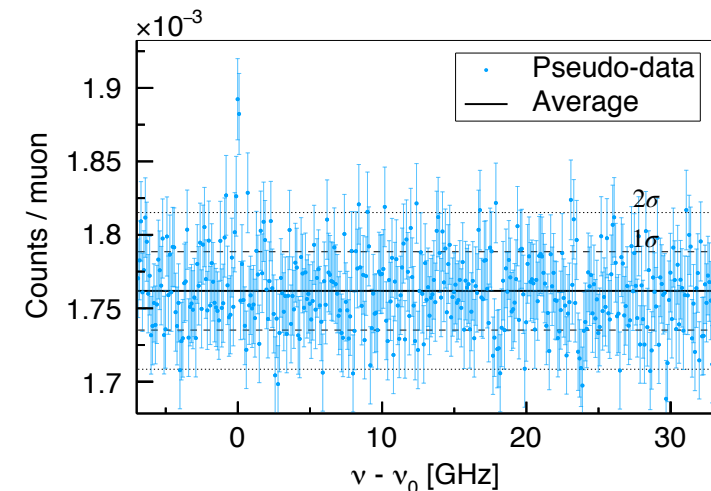


Search for the resonance



- **Steps to search for resonance**
- Measure 1.4 h at fixed wavelength to expose a 4σ effect over background
- 1 h to change the laser frequency in steps of 100 MHz

- **Simulation of the search for resonance**



Simulated resonance

Assuming the resonance has been found and given:

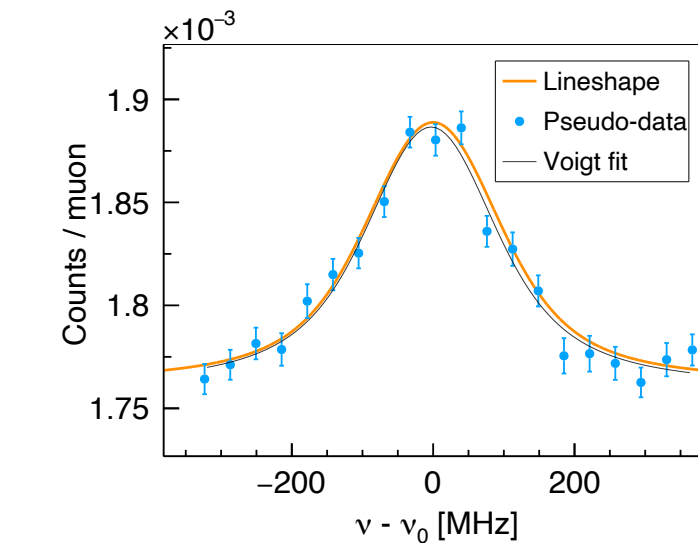
- Laser pulse 1mJ
- Target length 1.2 mm
- Cavity R = 99.2%
- Detection system: $\epsilon_{\text{Au}} = 70\%$, $\epsilon_{\text{Au-false}} = 9\%$



Determine resonance position with

$$\sigma = 4 \text{ MHz} (1.6 \times 10^{-8} \text{ eV})$$

$$\frac{\sigma}{E_{\text{HFS}}} = \frac{4 \text{ MHz}}{44 \text{ THz}} = 1 \times 10^{-7}$$



• Theory improvement needed

Collaboration



P. Indelicato, F. Nez, N. Paul, P. Yzombard



T.W. Hänsch



JOHANNES GUTENBERG
UNIVERSITÄT MAINZ

A. Ouf, R. Pohl,
S. Rajamohanam, F. Wauters



Yi-Wei Liu, L.-B. Wang, Yi-Jan
Tzu-Ling Chen, Wei-Lin Chen



L. Affoltern, D. Göldi, E. Gründeman, O. Kara, K. Kirch, F. Kottmann, J. Nuber,
K. Schuhmann, D. Taqqu, M. Zeyen, A. Antognini, M. Hildebrandt,
A. Knecht, M. Marszalek, L. Sinkunaite, A. Soter



P. Amaro, P.M. Carvalho, M. Ferro,
M. Guerra, J. Machado, J. P. Santos,
L. Sustelo



UNIVERSIDADE DE COIMBRA

F.D. Amaro, L.M.P. Fernandes,
C. Henriques, R.D.P. Mano,
C.M.B. Monteiro, J.M.F. dos Santos,
P. Silva



A. Adamczak



M. Abdou-Ahmed, T. Graf

Our lab at PSI



Questions

Questions ?